Special Issue Article

Advances in Mechanical Engineering

Advances in Mechanical Engineering
2017, Vol. 9(1) 1–11

DOI: 10.1177/1687814016681235
journals.sagepub.com/home/ade
SAGE

Parametrisation of a Maxwell model for transient tyre forces by means of an extended firefly algorithm

Andreas Hackl[1], Wolfgang Hirschberg[1], Cornelia Lex[1] and Christian Magele[2]

Abstract

Developing functions for advanced driver assistance systems requires very accurate tyre models, especially for the simulation of transient conditions. In the past, parametrisation of a given tyre model based on measurement data showed shortcomings, and the globally optimal solution obtained did not appear to be plausible. In this article, an optimisation strategy is presented, which is able to find plausible and physically feasible solutions by detecting many local outcomes. The firefly algorithm mimics the natural behaviour of fireflies, which use a kind of flashing light to communicate with other members. An algorithm simulating the intensity of the light of a single firefly, diminishing with increasing distances, is implicitly able to detect local solutions on its way to the best solution in the search space. This implicit clustering feature is stressed by an additional explicit clustering step, where local solutions are stored and terminally processed to obtain a large number of possible solutions. The enhanced firefly algorithm will be first applied to the well-known Rastrigin functions and then to the tyre parametrisation problem. It is shown that the firefly algorithm is qualified to find a high number of optimisation solutions, which is required for plausible parametrisation for the given tyre model.

Keywords

Vehicle dynamics, tyre dynamics, semi-physical tyre model, parameter optimisation, swarm optimisation, firefly algorithm, clustering, experimental validation

Date received: 3 June 2016; accepted: 31 October 2016

Academic Editor: Bin Yu

Introduction

Modelling and simulation of safety-relevant driver assistance systems (DASs) and vehicle dynamics controllers (VDCs) which act in standard and limit situations lead to increasing accuracy demands in the description of dynamic reactions of tyre contact forces, particularly with respect to the delayed response to transient control input. For this purpose, first-order approaches are widely applied in this field of vehicle dynamics and handling, which originate from Von Schlippe and Dietrich,[1] were modified by Pacejka[2] and were later on refined by Rill.[3]

In previous investigations, experimental validation showed that the first-order Kelvin–Voigt model, described by a spring and a damper elements, describes good suitability around fixed operation points but is limited for a wide working range.[4,5] When aiming to run vehicle dynamics models within a frequency band

[1]Research Area of Driver Assistance, Vehicle Dynamics and Suspensions, Institute of Automotive Engineering, Graz University of Technology, Graz, Austria
[2]Institute for Fundamentals and Theory in Electrical Engineering, Graz University of Technology, Graz, Austria

Corresponding author:
Andreas Hackl, Research Area of Driver Assistance, Vehicle Dynamics and Suspensions, Institute of Automotive Engineering, Graz University of Technology, Inffeldgasse 11/II, 8010 Graz, Austria.
Email: andreas.hackl@tugraz.at

of excitation up to 8 Hz, these models deliver remarkable deviations from measured tyre characteristics. To overcome this limitation, a non-linear Maxwell spring–damper element was introduced which is qualified to model the dynamic hardening of the elastomer materials of the tyre.[6] However, the advantage of a more realistic description of the transient behaviour leads to a more complex parametrisation process. In Hackl et al.,[6] an iterative method was presented, to find a possible set of values to parametrise the Maxwell model.

But in particular, any obtained set of the identified model parameters typically depends on the chosen testing procedure. Thus, it is worth not only to consider the global optimum which satisfies a certain objective function but also to study local optima with respect to their relevance on the overall validity of the model within its area of operation.

Therefore, in continuation of previous works as cited above, in this article attention is paid to find an alternative optimisation method to parametrise the mentioned Maxwell model in a way to gather parameter information instead of getting just one possible solution. Because focus will be held on the optimisation algorithm, just one working point of the tyre, for example, constant normal force F_Z, will be investigated in this article, see in more detail in section 'Test-bench set-up and measurement procedure'. Further investigations will be done to apply this parametrisation method on more influencing parameter.

The application of stochastic optimisation algorithms for the optimisation of technical design problems has become an established and approved approach over the last decades. Methods using simplified sequences of complex natural processes are among the most successful ones of this class. Unfortunately, their major advantages like numerical stability and high convergence rate are still followed by the high number of evaluations of the particular objective function. Despite the enormous increase in computation power, this inherent feature of stochastic methods may make them infeasible in case of problems with computationally 'expensive' forward problems. Therefore, a major goal of any improvement of stochastic methods is to extract as much information as possible from as few function calls as reasonable.

Prior investigations of the tyre parametrisation problem are extended using the firefly algorithm (FFA), which belongs to the so-called swarm-based metaheuristics.[7] Inherent to all these methods is the information transfer from individual to individual. In nature, fireflies are forming swarms by attracting other individuals using a kind of flash light.[7,8] The luminosity of a single firefly decreases radially. Since the total light intensity of a crowd of fireflies depends on the number of insects and their individual luminosity, this integral feature can advantageously be used to form fractions of swarms, which can be expected in the vicinity of locally optimum solutions.

Cluster algorithms such as the complete linkage algorithm,[9] can be exploited to boost the formation of these clusters and, therefore, boost the search strategy to local minima. Once a reasonable number of clusters have been found, the well-known update procedure of fireflies is performed inside a single cluster only for a few predefined iteration steps. Afterwards, the best solution of each cluster is stored, and clustering is performed again. To assess the performance of the enhanced firefly algorithm (eFFA), first the Rastrigin test function is used,[10] where numerous local solutions are found in the region of interest.

Finally, the eFFA is applied on the parametrisation problem of tyre model parameter identification based on measurements. This approach promises to faster provide a set of certain model parameters and covers the usual range of dynamic driving manoeuvres. In addition, the suitability of the used testing procedure for parameter identification can be evaluated.

Modelling transient tyre dynamics

With increasing level of complexity and also automation, the simulation of safety-relevant advanced driver assistance systems (ADASs) leads to increasing accuracy demands in the description of tyre contact forces.[11] This includes the consideration of dynamic effects, such as the delayed reaction in longitudinal and lateral tyre forces to dynamic changes in slip in the tyre-road contact patch. Often, this behaviour is characterised by a first-order differential equation which describes the deflection of particles in the tyre's tread by considering a spring and a damper elements in parallel.[3] Previous investigations showed that for some working points, these simple models show good compliance. However, when aiming to run vehicle dynamics models with an excitation frequency of up to 8 Hz, these models show deviations from measured characteristics.[5,6] To overcome this limitation, a dynamic tyre force model including a Maxwell element will be presented in the following for lateral tyre dynamics.

Tyre dynamics including Maxwell element

First-order approaches are widely applied in the field of vehicle dynamics to describe the transient behaviour of a tyre contact force. One model description is shown in Figure 1 on the left side.[3] A lateral force F_y acting in the contact patch leads to the lateral tyre deflection y_e. The resulting dynamic force can be described by a spring with the linear stiffness c_y in parallel to a damper with linear damping constant d_y, also known as Kelvin–Voigt model. Previous investigations have shown that this model works well during a fixed operating point

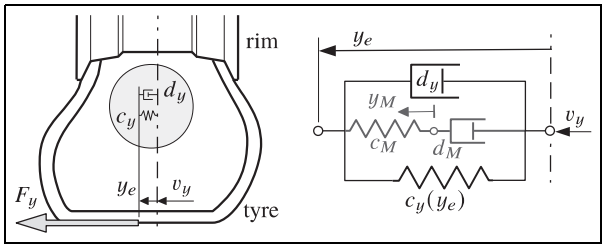

Figure 1. Simple tyre dynamics model for lateral direction (left) and Maxwell model for lateral tyre dynamics (right).[6]

but has some disadvantages on a wide manoeuvre range. Therefore, a model extension was implemented. At first, a linear spring is replaced by a non-linear one $c_y = c_y(y_e)$ by simply adding a term proportional to the tyre deflection.

Second, placing a Maxwell element consisting of a serial spring and damper element with constants c_M and d_M in parallel to the Kelvin–Voigt model leads to the so-called Maxwell model as shown in Figure 1 on the right side. The dynamic force F_y^D in the lateral direction is defined by the Taylor expansion

$$\begin{aligned} F_y^D &= F_y(v_y + \dot{y}_e) \approx F_y(v_y) + \frac{\partial F_y}{\partial v_y}\dot{y}_e \\ &= F_y^{st} + \frac{\partial F_y}{\partial s_y^N}\frac{\partial s_y^N}{\partial v_y}\dot{y}_e \end{aligned} \tag{1}$$

including the steady-state lateral tyre force F_y^{st} and the lateral component of the contact point velocity v_y. This relation is accompanied by the force law for the Maxwell model which is given by

$$F_y^D = c_y y_e + c_M(y_e - y_M) + d_y\dot{y}_e \tag{2}$$

A normalised lateral slip is used within the tyre model TMeasy that is defined by

$$s_y^N = \frac{-v_y}{r_D|\Omega|\hat{s}_y + v_N} \tag{3}$$

where v_y denotes the lateral component of the contact point velocity derived from the rim motions, r_D describes the dynamic rolling radius of the tyre, Ω defines the angular velocity of the wheel about the wheel rotation axis and $\hat{s}_y$ names a slip normalisation factor.[3] In addition, a small fictitious velocity $v_N > 0$ was added in the denominator to avoid singularities in the lateral slip when $\Omega = 0$ will occur at a locked wheel or at standstill. The TMeasy tyre model introduces a generalised three-dimensional tyre slip s_G where the normalised longitudinal and lateral slips as well as the bore slip are vectorially added. Then, a generalised tyre characteristic $F_G = F_G(s_G)$ is used to describe the steady-state tyre behaviour. As a consequence, the steady-state lateral tyre force and its partial derivative with respect to the normalised lateral slip are given by

$$F_y^{st} = \frac{F_G}{s_G}s_y^N = f_G s_y^N \quad \text{and} \quad \frac{\partial F_y}{\partial s_y^N} \approx f_G \tag{4}$$

where f_G characterises the global derivative of the generalised tyre characteristics F_G with respect to the generalised slip s_G. Combining equations (1) and (2) and taking equations (3) and (4) into account result in

$$\left(v_{Ty}^* d_y + f_G\right)\dot{y}_e = -v_{Ty}^* c_y y_e - v_{Ty}^* c_M(y_e - y_M) + f_G v_{Ty}^* s_y^N \tag{5}$$

where a modified transport velocity $v_{Ty}^* = r_D|\Omega|\hat{s}_y + v_N$ is used to simplify the expressions. In equation (5), the time derivative of the lateral tyre deflection y_e also depends on the stiffness c_M and the internal displacement y_M of the Maxwell element. Applying the force balance delivers a second first-order differential equation

$$d_M\dot{y}_M = c_M(y_e - y_M) \tag{6}$$

or

$$T_M\dot{y}_M = -y_M + y_e \tag{7}$$

where

$$T_M = \frac{d_M}{c_M} \tag{8}$$

driven by the lateral tyre deflection y_e and characterised by the time constant T_M, which is defined by the stiffness and damping parameters c_M and d_M.

Test-bench set-up and measurement procedure

The measurements have been conducted on a brake and suspension test rig, which was developed for investigations of durability and fatigue of components of quarter vehicle suspensions.[12] The test bench has a steel drum with a standardised outer diameter of 1.219 m. The drum tread has been flame sprayed with a chrome-steel alloy, resulting in a friction coefficient between drum and tyre of $\mu = 0.9$.[13] The drum can be pivoted around the vertical axis to generate a slip angle α. A rigid suspension without spring and damper elements was used to mount the wheel carrier to the test rig as shown in Figure 2. The resulting forces and torques in the wheel hub are measured using a high-precision Kistler-IGel wheel force transducer (WFT),[14] applied on a common radial car tyre size of 205/55 R16 with asymmetrical tread design.

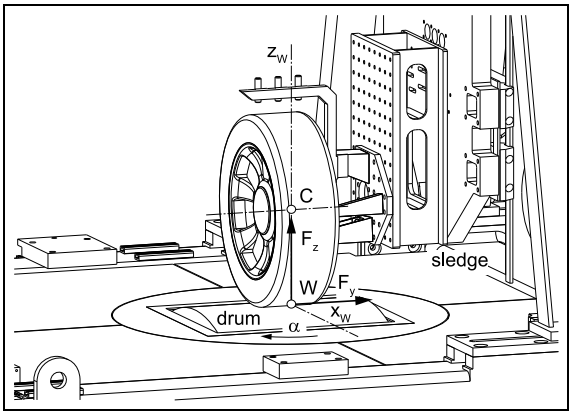

Figure 2. Drum test rig with wheel assembly.[6]

Table 1. Overview on measurement conditions.

Name	Value	Unit
Tyre load F_z	3600	N
Tyre pressure p_i	2.75	bar
Longitudinal velocity v_x	60	km/h
Wheel camber γ	0	°
Sine amplitude A_s	2	°
Sine frequency f_s	0.25, 0.5, 1, 1.5, 2, 2.5, 3, 3.5, 4	Hz

As mentioned in section 'Introduction', the focus of this article will be on the parametrisation algorithm. Therefore, one tyre condition with constant tyre load F_z, tyre pressure p_i and longitudinal velocity v_x is used. An overview on the measured values is given in Table 1. To investigate the frequency dependency, sine steer manoeuvres with different frequencies f_s were performed for the present investigations. In this dynamic manoeuvre, the slip angle α between wheel and the drum of the test rig is varied as a sinusoidal function with an amplitude $A_s = 2^\circ$ and is shown in Figure 3. For further investigations, the parametrisation process will be repeated with focus of the parameter behaviour for different conditions.

Optimisation strategy: FFA

In this study, a d dimension, bound constrained parametrisation problem using an eFFA is solved. The mathematical formulation of the optimisation problem to be solved is stated as follows

$$\min_{\mathbf{x}\in\mathbb{R}^d} f(\mathbf{x}) \quad \text{subject to} \quad \boldsymbol{l}_b \le x \le \boldsymbol{u}_b \tag{9}$$

where $f(\mathbf{x})$ is the Rastrigin test function in the first and the tyre dynamics parametrisation problem in the second case, with $\boldsymbol{l}_b$ and $\boldsymbol{u}_b$ as the lower and upper boundaries. For the tyre model parametrisation problem, the root-mean-square deviation (RMSD) between measurements and simulation was used. To compare different frequencies f_s, the RMSD was normalised additionally. Therefore, the mathematical description of the cost function for the parametrisation problem of the tyre model is mentioned as given by the normalised root-mean-square deviation (NRMSD) and defined as

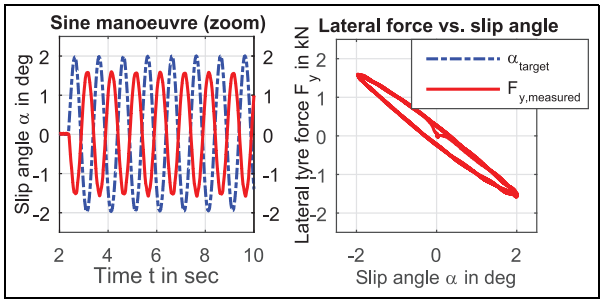

Figure 3. Sine steer manoeuvre target with measured lateral tyre force and a sine frequency of $f_s = 1$ Hz.

$$\mathrm{NRMSD} = \frac{\mathrm{RMSD}}{\widehat{F}^D_{y,max} - \widehat{F}^D_{y,min}} \tag{10}$$

and

$$\mathrm{RMSD} = \sqrt{\frac{\sum_{t=1}^{n} \left(\widehat{F}^D_{y,t} - F^D_{y,t}\right)^2}{n}} \tag{11}$$

where $\widehat{F}^D_{y,t}$ is defined as measured lateral force, with the maximum and minimum values $\widehat{F}^D_{y,max}$ and $\widehat{F}^D_{y,min}$, respectively; $F^D_{y,t}$ is the simulated force and n is the total length.

In the following, the original FFA from Yang[7] and the enhancements to find local minima with a higher probability are presented.

Original FFA

The foundation of the basic FFA is based on the natural inspired behaviour of fireflies. There are nearly 2000 different firefly species of which most produce short and rhythmic flashes. The rhythms and intensity of these flashes may be different, but they share two fundamental functions to attract mating partners and potential prey.

First, the intensity of light at a certain distance r from the light source conforms to the inverse square law. This means the intensity of light I decreases as the distance r increases in terms of $I \propto 1/r^2$. Second, the air absorbs light which becomes weaker with an increasing distance. These combined factors limit the distance of

communication of fireflies. With this information, a flashing characteristic to develop a firefly-inspired algorithm is idealised. FFA which was developed by Xin-She Yang[7,8] at Cambridge University in 2007 uses three idealised rules:

- All fireflies are unisex, so it means that one firefly is attracted to other fireflies irrespective of their sex.
- Attractiveness and brightness are proportional to each other, so for any two flashing fireflies, the less bright one will move towards the one which is brighter. Attractiveness and brightness both decrease as their distance increases. If there is no one brighter than any other firefly, it will move randomly.
- The brightness of a firefly is determined by the objective function.

This algorithm is based on two important issues: the variation of light intensity and formulation of the attractiveness. The light intensity I of firefly i, therefore I_i, depends on the initial intensity I_0 and the distance r between firefly i and j. In Yang,[7] the light intensity of I_i varies with the distance r_{ij} monotonically and exponentially with

$$I_i = I_0 \cdot e^{-\gamma r_{ij}} \tag{12}$$

where γ is the light absorption factor. Since the attractiveness β_{ij} of the firefly i is proportional to the light intensity seen by an adjacent firefly j and their distance r_{ij}, the attractiveness is given by

$$\beta_i = \beta_0 \cdot e^{-\gamma r_{ij}} \tag{13}$$

where β_0 is the attractiveness at $r_{ij} = 0$.

In the original FFA, the distance r_{ij} between any two fireflies i and j at their positions $\boldsymbol{x}_i$ and $\boldsymbol{x}_j$ could be given by the Cartesian distance (or 2-norm)

$$r_{i,j} = \| \boldsymbol{x}_i - \boldsymbol{x}_j \| = \sqrt{\sum_{k=1}^{d} \left(x_{i,k} - x_{j,k}\right)^2} \tag{14}$$

In summary, the movement of a firefly i towards another more attractive (brighter) firefly j is given by

$$\boldsymbol{x}_i = \boldsymbol{x}_i + \beta_0 e^{-\gamma r_{ij}} \left(\boldsymbol{x}_j - \boldsymbol{x}_i\right) + \alpha \varepsilon_{ij} \tag{15}$$

where the second term is due to the attraction of two flies, described in equation (13). The third term is a randomisation with α being the randomised parameter and ε_{ij} is a random vector generated from a Gaussian or uniform distribution. For simplest implementation, ε_{ij} can be replaced by $rand - (1/2)$, where $rand$ is a randomly generated number between [0, 1].

With this presented algorithm, quite a lot of optimisation problems can be solved with parameter selection of α, γ and $\beta_0 = \mathcal{O}(1)$. However, in a single iteration step, each individual has to be compared with all others in the population and followed by an immediate update of its position, as shown in equation (15), and a subsequent evaluation of the quality for its position. Using the Rastrigin test functions, it can be seen that the basic FFA already tends to cluster the population around more or less local solutions, but this property depends to a high level on the specified parameters.

Modified firefly approach

For many application problems, the boundaries to solve optimisation problem are different to mathematical functions. On one hand, computational effort is limited; therefore, especially for complex objective functions, each function call costs calculation time which automatically means costs. On the other hand, the globally best solution is not always the technically best solution. Furthermore, it is not so important to find the global/local minima quite exactly. Often, it is more important to focus calculation power on definition of minima regions with a high probability, because the final decision is taken from technical considerations anyway.

Therefore, the focus of the presented enhancement of the FFA was put on three main goals:

1. Minimisation of the number of function calls to reduce optimisation time;
2. Strong search focus on local minima to evaluate a high number of technically feasible solutions;
3. Increase stability of the algorithm to fulfil the first two goals on different optimisation problems, with a minimum dependency of the firefly parameters.

The basic FFA calculates the new value of the objective function after each particle movement. This may be quite effective because each particle gets a new position and also a new function value, where other particles can focus on, but the number of function calls is quite high. The maybe easiest and most effective simplification to save function calls is to resign to calculate a new objective value after each particle movement and update new values of the swarm after the movement of the whole swarm only. A disadvantage of this method is that some particles may focus on a new position with old function values. This possibility increases with a higher number of fireflies. Decreasing the number of particles below a certain threshold does not work for most optimisation problems. Therefore, a different solution had to be found to minimise the error of subsequent function calls.

Algorithm 1: Enhanced Firefly Algorithm

Define objective function $f(\boldsymbol{x})$, $\quad \boldsymbol{x} = (\boldsymbol{x}_1, \ldots, \boldsymbol{x}_d)^T$
Generate init. population of m fireflies $\boldsymbol{x}_i$ $(i = 1, \ldots, m)$
Define FA parameters γ, β_0 and α
Determine light intensity I_i at $\boldsymbol{x}_i$ via $f(\boldsymbol{x}_i)$
while (t <MaxGeneration it_{max})
Clustering population in (new) l clusters
for $k1 = 1 : l$, for each cluster $1, \ldots, l$
  for $k2 = 1 : n$, run FA n-times (with $n < t$)
    for $i = 1 : m'$, all m' fireflies depending on $k1$
      for $j = 1 : m'$, all m' (inner loop)
      if $(I_i < I_j)$
        Move firefly i towards j using in equation (13)
      end if
      end for j
    end for i
    Evaluate new solutions and update light intensity
    $I_{1\ldots m'}$ for each firefly $\boldsymbol{x}_{1\ldots m'}$ in cluster $k1$
  end for $k2$
  Rank the fireflies in cluster $k1$
  Save cluster best $\boldsymbol{x}_{local}$
end for $k1$
Rank all fireflies and find the current global best $\boldsymbol{g}_*$
end while
Postprocess results and visualisation

Figure 4. Pseudo code of the enhanced firefly algorithm.

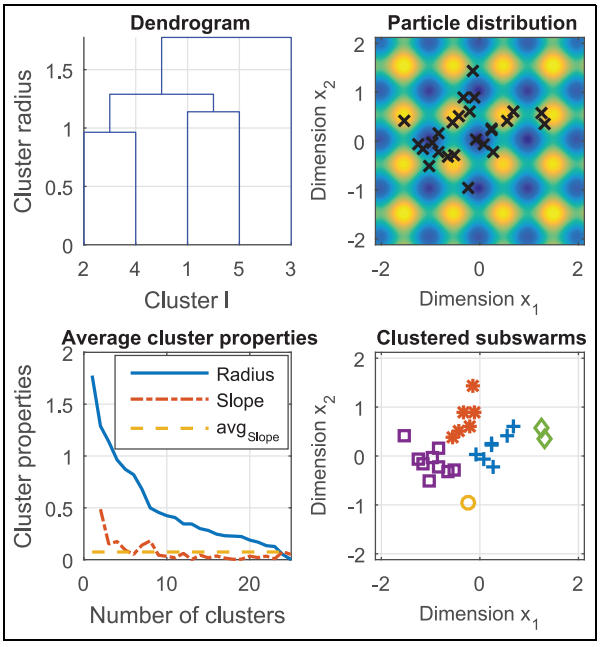

Figure 5. Clustering process (two left sub-figures) and the particle distribution with the clustered at iteration step $it = 12$ of maximal $it_{max} = 24$ iteration runs.

After n iterations, the population is clustered hierarchically using complete linkage.[9] Some metric depending on the size of the cluster radii is used to determine suitable number of clusters. Then, FFA update is performed within clusters only. After this, the best solution of each cluster is stored and analysed after the final iteration step. This extension reveals two advantages. First, it reduces the number of unsuccessful movements considerably, and second, it tends to find a remarkable number of local solutions.

The strategy parameter of the FFA is chosen in dependency on the optimisation boundary with reference to Yang[15] and presented in the next section. A pseudo code of the eFFA is summarised in Figure 4.

Results

After defining the optimisation strategy, first the algorithm behaviour is tested and discussed on the well-known two-dimensional Rastrigin function and afterwards applied to the tyre parameter identification problem using test-bench measurements.

Rastrigin function

To be sure to find the global solution with a high probability, as well as to find good local solutions for different optimisation problems and additionally use the same parameter configuration for both optimisation problems, the FFA parameters are chosen with respect to the given boundary conditions. $\boldsymbol{L}$ describes the space between upper and lower boundaries with $\boldsymbol{L} = \boldsymbol{u}_b - \boldsymbol{l}_b$ for each dimension. Therefore, the absorption coefficient is defined with $\gamma = 0.75/(\sqrt{\boldsymbol{L}} \cdot \| \boldsymbol{b} \|_2)$, where $\boldsymbol{b} = [\boldsymbol{l}_b, \boldsymbol{u}_b]$, and the random factors $\alpha = 0.75\boldsymbol{L}$. Usually, this coefficient is updated in every iteration step by $\alpha^{t+1} = \alpha^t \delta$, where the factor δ is chosen as a 'randomness reduction' with $\delta = 0.9$. This definition of the three parameters allows an easy scaling between 0 and 1, for example, for the randomness factor between $\alpha = 0 \cdot \boldsymbol{L}$ (no random part) and $1 \cdot \boldsymbol{L}$ (high random part).

The population consists of $m = 25$ individuals and $it_{max} = 24$ iterations, where after $n = 4$ runs, the population is re-clustered. In summary, this means 600 function calls with 6 clustering processes in total. In Figure 5, the algorithm behaviour after $it = 12$ of $it_{max} = 24$ iterations is presented. On the left two subfigures, the clustering process is presented, whereas on the bottom cluster radius, cluster slope and average slope per number of clusters are shown. It can be seen that with a higher number of clusters, the average cluster radius decreases until the minimum of zero is reached, which means each particle has its own cluster. Depending on the slope of the cluster radius, the number of clusters for the next $n = 4$ iteration steps is chosen. The highest number of clusters whose slope is higher than the average cluster slope determines the number of clusters. In this case, five clusters were

Table 2. Found number of global minima and number of found local minima during 100 algorithm runs.

Runs	Global	Local					
		≥10	9	8	7	6	≤5
100	82	4	13	21	38	17	7

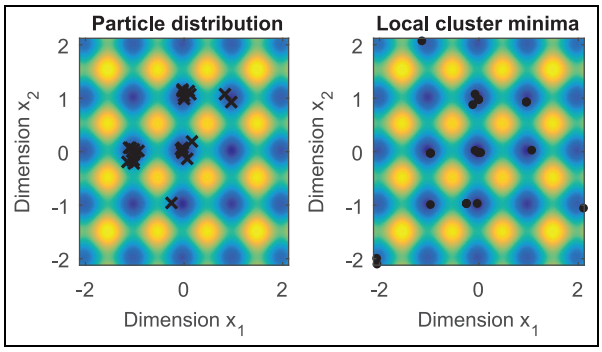

Figure 6. Final FFA particle distribution (left) and the found local minima during clustering (right) with $m = 25$ particles and $it_{max} = 24$ iteration runs.

chosen with an average cluster radius of $r_{avg,l} \approx 0.5$, where each cluster l_i with $i = 1, \ldots, 5$ has a different number of fireflies m' in its cluster.

On the upper left sub-figure of Figure 5, the dendrogram, which presents the cluster radius depending on the number of clusters, and the membership of the sub-clusters and particles are shown. If a lower number of clusters would be chosen, first cluster 2 and cluster 4 join; afterwards cluster 1 and cluster 5; and in the end, a single cluster with the radius ≈ 1.75 is left. For the sake of retaining an overview, just the clustering up to five clusters is printed.

On the two right sub-figures, the swarm behaviour is presented, whereby on the upper one, the swarm particles are shown together with the contours of the Rastrigin function, and on the bottom, the particles are shown in their clustered sub-swarms. For the next four steps, each sub-swarm has its own behaviour and finds different minima.

In Figure 6, the firefly behaviour after the final step is presented. It can be seen that with the final flies characteristic, shown on the left sub-figure, the algorithm was able to find the global minimum in this case and additional three other minima.

In comparison, with the help of all local minima, saved before new clustering, it was possible to find nine areas of local minima and one output which is not directly in a minimum, see $x_{bad} = [-0.15, -1]$. Therefore, just with saving intermediate results, the number of local minima detected was increased in a high level.

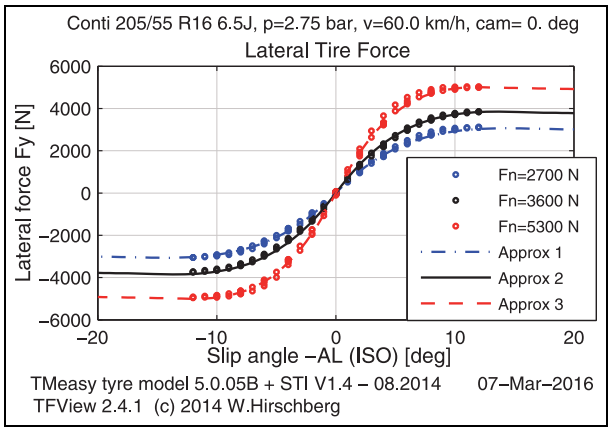

Figure 7. Parametrisation of the steady-state tyre model TMeasy using the utility software *TFView*.[6]

Regarding the firefly x_{bad}, it can be seen in the bottom right sub-figure of Figure 5 that there is one cluster with just one fly, see firefly o. Because of the adapted algorithm, the best fly of each cluster does not move and is stored for $n = 4$ iteration steps. This means, the position of x_{bad} is stored as well and found in the final results, see Figure 6. This behaviour will be changed in the next version of the algorithm.

To investigate the stability of the eFFA, a test procedure with 100 test runs was done to validate the average of found global minima and the number of found local minima. The results are presented in Table 2. Exemplarily, in 82 of 100 runs, the global minimum was found, and only in 4 of 100 runs, ≥10 local minima were found additionally.

Parametrisation of the non-linear tyre dynamic approach

As shown before, for the Rastrigin function, the eFFA was able to find the global minimum and local minima. Now, the same strategy, with the same parameters, is used to solve the parametrisation problem of the non-linear tyre dynamic approach described in section 'Modelling transient tyre dynamics'.

Before starting to parametrise and validate the dynamic tyre behaviour, a steady-state tyre model is required. This characteristic is parametrised with slip angle step steer inputs of $\alpha = \{1, 2 \text{ and } 4\}^{\circ}$ at a constant drum speed of 60 km/h, as shown in Figure 7. The circles symbolise the measurement points and the lines the parametrised model TMeasy. The parametrisation of the steady-state characteristic is supported by the utility software *TFView*[16] and described in detail in Hackl et al.,[6] for general information, see Rill.[3]

To alleviate the optimisation problem, the non-linear characteristic of the spring $c_y(y_e)$ is parametrised

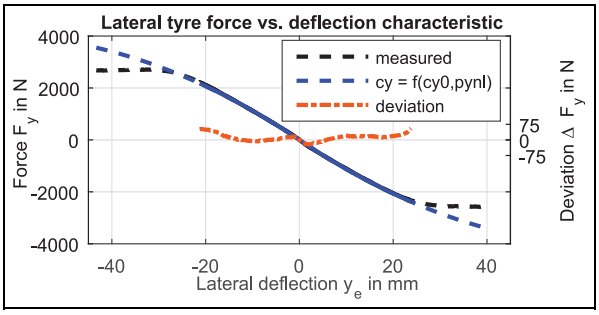

Figure 8. Comparison of the identified non-linear lateral spring characteristics and the measurement data.[6] Estimated parameters: $c_y = 121,819\,\mathrm{N\,m}$ and $p_y = -7.5466/\mathrm{m}$.

in a previous step. The focus of this optimisation was put on the parameters of the model that influence the dynamic behaviour. Furthermore, the non-linear behaviour of the spring $c_y(y_e)$ just influences the force characteristic on manoeuvres with higher slip angles α which is equal to a higher lateral deflection y_e. Further measurements with higher slip angle $\alpha \gg 2^\circ$ are planned to investigate the optimisation characteristics and parametrise the model during one optimisation step.

For parametrisation of the non-linear characteristics, a lateral displacement y_e was produced and the lateral force F_y measured. Because of the very slow lateral movement, a quasi-stationary behaviour was assumed. Therefore, with $c_y(y_e) = c_y \cdot (1 + p_y|y_e|)$, equation (2) becomes

$$F_y^S = c_y y_e + c_y p_y |y_e| y_e \tag{16}$$

where F_y^S describes the quasi-stationary lateral tyre force. In Figure 8, the results of the modelled non-linear spring, determined with the least square method, is presented. It can be seen that in the interested area (solid line), the deviation is less than about 50 N. For detailed information, see Hackl et al.[5,6]

Finally, the damper d_y and the two Maxwell element parameters c_M and d_M have to be found with the eFFA. Therefore, the measured and simulated lateral forces are compared and optimised to a minimum NRMSD. Because of the lacking knowledge about the area of the Maxwell parameter, a large range was used for the optimisation, see Figure 9. To find the parameter areas depending on the different frequencies from Table 1, each frequency was optimised and investigated separately. In Figure 9, parametrisation results for four different frequencies $f = \{1, 2, 3, 4\}\,\mathrm{Hz}$ are presented. On the upper sub-figure, the final firefly position after $it_{max} = 24$ iteration steps and in the lower one the local minima found during clustering are presented, with respect to a lower cost function than the state-of-the-art Kelvin–Voigt model, see Table 5. It can be seen that in

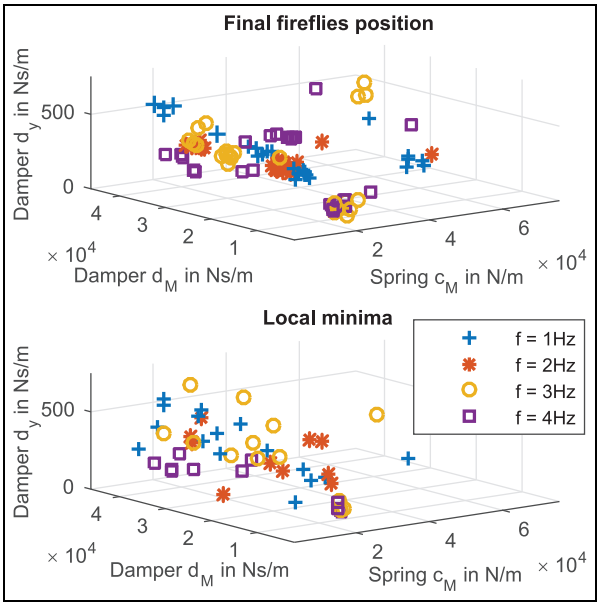

Figure 9. Parameter results of one eFFA run with $it_{max} = 24$ iterations, $m = 25$ fireflies and clustering after $n = 4$ iterations.

the final positions as well as in the local minima, two main areas (MAs) with a high population density and two sub-areas (SAs), especially in the local minima plot, are grouped. A rough parametrisation description of these four areas is shown in Table 3.

It can be seen in Table 3 that the deviation of the Maxwell damper d_M is in a higher range than the Kelvin–Voigt damper d_y and the Maxwell spring c_M. This confirmed the investigations of previous parametrisation with the particle swarm optimisation (PSO), published in Hackl et al.[6] To reduce this deviation, focus for future investigations will be held on different measurement manoeuvres, which is equal to an improvement of the cost function. Furthermore, other extensions for future investigations are to investigate the whole frequency range during one optimisation run, to weight separate frequencies to keep focus on a preferred range, such as in Alb et al.,[17] or to transform the optimisation problem to a multi-objective problem for each frequency.

Based on the results from the eFFA optimisation, area MA 1 was chosen for investigation in the present article, which means the upper boundary for $[d_y, c_M, d_M] \leq [750\,\mathrm{N\,s/m}, 30,000\,\mathrm{N/m}, 15,000\,\mathrm{N\,s/m}]$. Three exemplary local minima found in these boundary conditions during maximal two optimisation runs, per each frequency, are presented in Table 4.

It can be seen from Table 4 that with the exception of very few outliers, the deviation is less than $\pm 10\%$ of the average c_M in Table 5, independent of the frequency. Alternatively, the Kelvin–Voigt damper d_y and the Maxwell damper d_M show a decreasing parameter

Table 3. Roughly found parameter areas with respect to the final firefly position and the found local minima during clustering.

Area	d_y (N s/m)	c_M (N/m)	d_M (N s/m)
MA 1	270	18,000	6,000
MA 2	300	20,000	36,000
SA 1	380	22,000	19,000
SA 1	290	33,000	30,000

MA: main area; SA: sub-area.

Table 4. Local minima during optimisation for each frequency $f = \{0.25, \ldots, 4\}$ Hz separately, found around MA 1.

Frequency (Hz)	d_y (N s/m)	c_M (N/m)	d_M (N s/m)
0.25	218	27,057	7194
	278	14,671	11,731
	225	21,154	10,659
0.5	511	20,724	9112
	230	23,894	9457
	558	26,750	6941
1.0	333	18,740	12,367
	267	19,436	11,170
	310	26,151	8023
1.5	287	19,165	10,764
	484	19,771	5666
	520	14,933	6092
2.0	260	21,560	8484
	331	20,321	8208
	579	15,564	5519
2.5	223	20,345	4798
	244	21,075	5905
	294	17,123	7026
3.0	133	19,879	4490
	122	20,193	5331
	181	19,689	5263
3.5	111	17,323	6645
	227	20,206	9690
	242	20,656	6130
4.0	143	18,373	4539
	181	18,077	4557
	85	22,752	7382

value in average per increasing frequency, on one hand, and a high deviation per found fly, on the other hand. The high deviation per found firefly and frequency are maybe traceable in the low slip angle amplitude of the manoeuvre, which could mean the influences of the damper decrease with smaller side slip angle α. Further investigations are planned to confirm these assumptions.

In total, the mean average of these three parameters d_y, c_M and d_M over the whole frequency range presented in Table 4 is calculated and summarised in Table 5. The simulation with the final Maxwell parameters, presented in Table 5 row MW, are compared with the state-of-the art Kelvin-Voigt model from Hackl et al.[6] and with the measurements. The comparison is presented in Figure 10.

In the two upper sub-figures of Figure 10, the characteristics of the lateral force during a sine manoeuvre with a frequency of $f = 2.5$ Hz is shown. On the right sub-figure, it can be seen that the behaviour of the Maxwell model $F_{y,MW}$ has a higher stiffness than the state-of-the-art Kelvin–Voigt model $F_{y,VK}$ which reduces to the dynamic hardening of the tyre stiffness on higher frequencies.

The bottom sub-figure shows the NRMSD of the sine manoeuvre with different frequencies. It can be seen that the errors of the Kelvin–Voigt increase with higher frequencies, and the errors of the Maxwell model are smaller for frequencies higher than about $f = 0.5$ Hz. This means, on one hand, that the Maxwell model describes the dynamic behaviour with a higher accuracy and, on the other hand, the parameters found in MA 1 with the eFFA are a good parametrisation solution for the Maxwell model.

Conclusion

The development of ADASs requires more accurate tyre models, especially for the simulation of transient driving conditions. However, a more realistic description of the transient behaviour leads to a more complex

Table 5. Final Maxwell (MW) model parameterisation found from the minima area MA 1 and compared with the state-of-the-art Kelvin–Voigt (KV) model parametrised in Hackl et al.[6]

Model	c_y (N/m)	p_y (1/m)	d_y (N s/m)	c_M (N/m)	d_M (N s/m)
MW	121,819	−7.547	281	19,910	7,535
KV	121,819	–	332	–	–

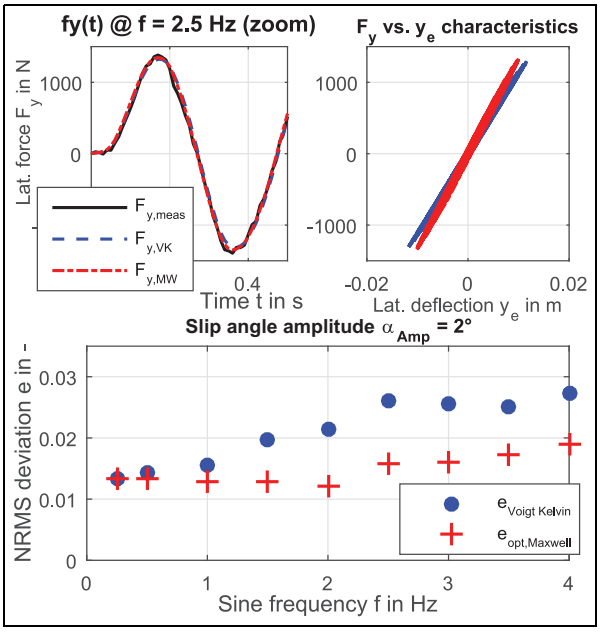

Figure 10. Results of the parametrisation of the tyre model, comparing measurements and the Kelvin–Voigt model. Above, comparison of the parametrised models with a measured sine manoeuvre with a frequency of $f = 2.5$ Hz and slip angle amplitude of 2°. Below, influence of different sine slip angle frequencies to the results of the NRMSD.

parameterisation process. Therefore, for this purpose, an eFFA was presented, which was used to find areas of local minima with only a few function calls. It was shown that the additional cluster algorithm boosts the search strategy to find a wide range of local minima, which means spend calculation time on parameter quantity in a first step. In a second step, preferred solutions can be chosen and investigated in more detail. This leads, on one side, to a good overview of the parameter areas for the optimisation problem and, on the other side, to a good ratio of acceptable solutions versus calculation time. Summarising, the eFFA is a robust and stable method to parametrise a wide range of optimisation problems.

Additionally, it is shown that the found parametrisation results are qualified to describe the dynamic tyre behaviour over a wide frequency range. It may also support the process of detecting suitable test-bench procedures with respect to the best model parametrisation. Summarising, the Maxwell element proved to be a suitable model element to describe the dynamic hardening of the viscoelastic materials of the rotating tyre. The presented work may be seen as one step towards the entire tyre dynamics modelling problem. In further investigations, possible influences like the tyre load have to be considered, to be able to cover the full operating range of a tyre. In addition, transient effects in longitudinal direction will be investigated to complete this research topic.

Acknowledgements

Andreas Hackl especially thanks Georg Rill for the support regarding the tyre model TMeasy and during the parametrisation process; Liang Shao and Martin Schabauer for the technical support and discussion within the research group; and Stefan Bernsteiner, Andreas Podlipnig and Anton Sternat for support during planning and conducting the measurements on the laboratory test bench. Costs for measurements were paid by the Institute of Automotive Engineering, Graz University of Technology, thanks to a strategic internal project.

Declaration of conflicting interests

The author(s) declared no potential conflicts of interest with respect to the research, authorship, and/or publication of this article.

Funding

The author(s) disclosed receipt of the following financial support for the research, authorship, and/or publication of this article: This work was supported by TU Graz Open Access Publishing Fund.

References

1. Von Schlippe B and Dietrich R. *Zur Mechanik des Luftreifens*. Berlin-Adlershof, Germany: Zentrale für wissenschaftliches Berichtswesen der Luftfahrtforschung (ZWB), 1942.
2. Pacejka HB. *Tire and vehicle dynamics*. Oxford: Butterworth-Heinemann, 2006.
3. Rill G. First order tire dynamics. In: *III European conference on computational mechanics solids, structures and coupled problems in engineering*, Lisbon, Portugal, 5–8 June 2006. Netherlands: Springer. DOI: 10.1007/1-4020-5370-3_776.
4. Hackl A, Hirschberg W, Lex C, et al. Tyre dynamics: model validation and parameter identification. In: *Proceedings of the EAEC-ESFA congress Bucharest 2015*, Bucharest, 25–27 November 2015. New York: Springer International Publishing.
5. Hackl A, Hirschberg W, Lex C, et al. Experimental validation of a non-linear first-order tyre dynamics approach. In: *Proceedings of the 24th symposium of the international association for vehicle system dynamics (IAVSD 2015)*, Graz, 17–21 August 2015, pp.443–452. London: Taylor & Francis Group, 2016. ISBN: 978-1-138-02885-2.
6. Hackl A, Hirschberg W, Lex C, et al. Experimental validation of the Maxwell model for description of transient tyre forces. In: *16th Stuttgart international symposium: automotive and engine technology*, Stuttgart, 15–16 March 2016, vol. 1, pp.401–418. Fachmedien Wiesbaden: Springer Vieweg. DOI: 10.1007/978-3-658-13255-2_29.

7. Yang XS. *Nature-inspired metaheuristic algorithms*. 2nd ed. Frome, UK: Luniver Press, 2010. ISBN-13: 978-1-905986-28-6.
8. Yang XS. Firefly algorithms for multimodal optimization. In: Watanabe O and Zeugmann T (eds) *Stochastic algorithms: foundations and applicants (SAGA 2009, lecture notes in computer sciences)*, vol. 5792. Berlin, Heidelberg: Springer-Verlag, pp.169–178.
9. Aichholzer O, Aurenhammer F, Brandstaetter B, et al. Evolution strategy and hierarchical clustering. *IEEE T Magn* 2002; 38: 1041–1044.
10. Rastrigin Function. Virtual library of simulation experiments: test functions and datasets, 2016, http://www.sfu.ca/~ssurjano/rastr.html (accessed 25 May 2016).
11. Hirschberg W, Weinfurter D and Jung C. Ermittlung der Potenziale zur LKW-Stabilisierung durch Fahrdynamiksimulation. In: *VDI-Berichte 1559*, 14–15 September 2000, pp.167–188. Düsseldorf: VDI-Berichte.
12. Harrich A, Tonchev A and Hirschberg W. Der neue dynamische Bremsen- und Radaufhängungsprüfstand an der TU Graz. In: *Proceedings of brake.tech*, Munich, 7–8 December 2006. Germany: TÜF Süd.
13. RENK Test Systems. *Schwungmassen-Bremsen-Prüfstand (SM-Brems-PS)*. Internal report, volume: 1/16, Document number: 4000069-TSD-ME-DE, Augsburg, Germany: Renk Test System GmbH, 2006.
14. Kistler GmbH. *RoaDyn® S635 System 2000*, 2015, https://www.kistler.com/?type=669&fid=39214&model=document (accessed 30 May 2016).
15. Yang XS. Multiobjective firefly algorithm for continuous optimization. *Eng Comput* 2013; 29: 175–184.
16. Hirschberg W, Rill G and Weinfurter H. Tire model TMeasy. *Vehicle Syst Dyn* 2007; 45(Suppl. 1): 101–119.
17. Alb M, Alotto P, Magele C, et al. Firefly Algorithm for finding optimal shapes of electromagnetic devices. *IEEE T Magn* 2015; 52(3). DOI: 10.1109/TMAG.2015.2483058.